Astron. Astrophys. 327, 620–635 (1997)

ASTRONOMY AND ASTROPHYSICS

# Stability criteria for mass transfer in binary stellar evolution

**G. E. Soberman**[1], **E.S. Phinney**[1], **and E.P.J. van den Heuvel**[2]

[1] Theoretical Astrophysics, 130-33 California Institute of Technology, Pasadena, CA 91125, USA
[2] Astronomical Institute and Center for High Energy Astrophysics (CHEAF), University of Amsterdam, Kruislaan 403, 1098 SJ Amsterdam, The Netherlands

Received 18 December 1996 / Accepted 26 May 1997

**Abstract.** The evolution of a binary star system by various analytic approximations of mass transfer is discussed, with particular attention payed to the stability of these processes against runaway on the thermal and dynamical timescales of the mass donating star. Mass transfer in red giant - neutron star binary systems is used as a specific example of such mass transfer, and is investigated. Hjellming & Webbink's (1987) results on the dynamic timescale response of a convective star with a core to mass loss are applied, with new results.

It is found that mass transfer is usually stable, as long as the wind's specific angular momentum does not exceed the angular momentum per reduced mass of the system. This holds for both dynamical and thermal timescales. Those systems which are not stable will usually transfer mass on the thermal timescale. Included are graphs illustrating the variation of $\frac{\partial \ln r_L}{\partial \ln m} \equiv \zeta_L$ with mass ratio in the binary, for various parameters in the non-conservative mass transfer, as well as evolutionary paths of interacting red giant neutron star binaries.

**Key words:** close binaries – tidal interaction – mass transfer

## 1. Introduction

The dominant feature in the evolution of stars in tight binaries, and the one which distinguishes it from the evolution of single stars is the presence of various forms of mass transfer between the two stars. Mass transfer occurs in many different types of systems, to widely varying effects (cf.: Shore 1994): contamination of the envelope of a less evolved star with chemically processed elements, as in Barium stars; winds from one star, which may be visible as a screen in front of the other, as in EM Car, AO Cas, and most notably the binary PSR 1259-63 (Johnston et al. 1992; Kochanek 1993; Melatos et al. 1995; Johnston et al. 1995); catastrophic mass transfer, by common envelope phase, as in W UMa systems; or a slow, steady mass transfer by Roche lobe overflow (RLOF).

Mass transfer is particularly interesting if one considers the evolution of a system with at least one degenerate star. In these cases, mass transfer produces spectacular effects, resulting in part from the intense magnetic and gravitational fields of the compact objects – pulsed X-ray emission, nuclear burning, novae outbursts, and so on. Also, since the mass transfer rates can be high, and orbital period measurements accurate, one may see the dynamical effects of mass transfer on the binary orbit, as in Cygnus X-3 (van Kerkwijk et al. 1992; van den Heuvel 1994).

In the case of cataclysmic variables (CVs) and low mass X-ray binaries (LMXBs), one has a highly evolved, compact star (CVs and LMXBs contain white dwarfs and neutron stars, respectively) and a less evolved main sequence or red giant star. Mass transfer usually proceeds by accretion onto the compact object, and is secularly stable. The transfer may be accompanied by a stellar wind from the mass-losing star, or ejection of matter from the accretor, as in novae and galactic jet sources.

There are various unanswered questions in the evolution of LMXBs into low mass binary pulsars (LMBPs, in which a millisecond radio pulsar is in a binary with a low mass white dwarf companion) and of CVs. Among these are the problem of the disparate birthrates of the LMXBs and the LMBPs (Kulkarni & Narayan 1988), estimation of the strength of X-ray heating induced winds from the donor star (London et al., 1981; London & Flannery 1982; Tavani & London 1993; Banit & Shaham 1992), effects of X-ray heating on the red giant structure (Podsiadlowski 1991; Harpaz & Rappaport 1991; Frank et al. 1992; Hameury et al. 1993), et c.

The problem of mass transfer in binaries by Roche lobe overflow has received a good deal of attention in the literature over the past few decades, typically in investigations of one aspect or another of orbital evolution or stability. Ruderman et al. (1989) examined mass transfer by isotropic winds and accretion, in investigating the evolution of short period binary X-ray sources with extreme mass ratios, such as PSR 1957+20 and 4U1820-30. King & Kolb (1995) developed models with

*Send offprint requests to*: G. E. Soberman; Internet Address: soberman@tapir.Caltech.EDU

accretion and (typically) isotropic re-emission of transferred matter, in the context of the period gap in cataclysmic variables.

The aim of this paper is to present a unified treatmant of binary orbital evolution and stability, with relevant equations in a general form. The limits of pure modes of mass transfer and extreme mass ratios are presented and examined, to gain a qualitative understanding of slow, non-disruptive mass transfer in its various forms.

The paper is organised as follows. Kinematic equations for orbital evolution, assuming mass transfer through some well-specified mode(s), are derived in Sect. (2). Conditions for and regions of stability are derived in Sect. (3). The theory is applied to LMXBs in Sect. (4), and conclusions drawn in the final section. Two appendices contain further details on the unified models and on comparisons among the various limits of the models.

## 2. Mass transfer and the evolution of orbital parameters

In this section, expressions for the variation of orbital parameters with loss of mass from one of the stars are derived. In what follows, the two stars will be referred to as $m_1$ and $m_2$, with the latter the mass losing star.

A binary composed of two stars with radii of gyration much less than the semimajor axis $a$ will have an angular momentum:

$$L = \mu \frac{2\pi}{P} a^2 (1-e^2)^{1/2} \,, \tag{1}$$

where the period $P$ is related to $a$ and the total mass $M_T = m_1 + m_2$ through Kepler's law:

$$GM_T = a^3 \left(\frac{2\pi}{P}\right)^2 \,. \tag{2}$$

Here, the reduced mass $\mu = m_1 m_2 / M_T$, the mass ratio $q = m_2/m_1$, and $e$ is the eccentricity. Tidal forces circularise the orbits of semidetatched binaries on timescales of $10^4 \mathrm{y} \ll \tau_{nuc}$,[1] the nuclear timescale on which the binaries evolve (Verbunt & Phinney 1995). Furthermore, one expects stable mass transfer by RLOF to circularise orbits. Consequently, an eccentricity $e = 0$ will be assumed for the remainder of this work.

Eqs. (1) and (2) combine to give expressions for the semimajor axis and orbital period, in terms of the masses and angular momentum:

$$a = \left(\frac{L}{\mu}\right)^2 (GM_T)^{-1} \,, \tag{3}$$

$$\frac{P}{2\pi} = \left(\frac{L}{\mu}\right)^3 (GM_T)^{-2} \,, \tag{4}$$

with logarithmic derivatives:

$$\partial \ln a = 2\,\partial \ln (L/\mu) - \partial \ln M_T \,, \tag{5}$$

$$\partial \ln P = 3\,\partial \ln (L/\mu) - 2\,\partial \ln M_T \,. \tag{6}$$

[1] In the usual case where the tidal timescale is also much shorter than the timescale of angular momentum loss by gravitational wave radiation, binaries in which mass transfer is driven by angular momentum loss are also tidally locked.

There are various modes (or, borrowing from the terminology of nuclear physics, channels) of mass transfer associated with the different paths taken by, and destinations of mass lost from $m_2$.

The details of mass transfer must be considered, in order to calculate the orbital evolution appropriate to each mode. Several of these modes are described here, roughly following Sect. 2.3 of the review article by van den Heuvel (1994).

The mode which is most often considered is accretion, in which matter from $m_2$ is deposited onto $m_1$. The accreted component (slow mode) conserves total mass $M_T$ and orbital angular momentum $L$. In the case considered here, of a Roche lobe filling donor star, matter is lost from the vicinity of the donor star, through the inner Lagrangian point, to the vicinity of the accretor, about which it arrives with a high specific angular momentum. If the mass transfer rate is sufficiently high, an accretion disk will form (cf: Frank, King, and Raine 1985). The disk forms due to viscosity of the proffered fluid and transports angular momentum away from and mass towards the accretor. As angular momentum is transported outwards, the disk is expands to larger and larger circumstellar radii, until significant tides develop between the disk and the mass donor. These tides transfer angular momentum from the disk back to the binary and inhibit further disk growth (Lin & Papaloizou 1979). The mass transfer process is conservative if all mass lost from the donor ($m_2$) is accreted in this way.

The second mode considered is Jeans's mode, which van den Heuvel calls, after Huang (1963), the fast mode; the third is isotropic re-emission. Jeans's mode is a spherically symmetric outflow from the donor star in the form of a fast wind. The best known example of Jeans's mode: the orbital evolution associated with Type II supernovae in binaries (Blaauw 1961) differs markedly from what is examined here. In that case, mass loss is instantaneous. A dynamically adiabatic outflow ($m/\dot{m} \gg P_{orb}$) is considered here.

An interesting variant of Jeans's mode is isotropic re-emission. This is a flow in which matter is transported from the donor star to the vicinity of the accretor, where it is then ejected as a fast, isotropic wind. The distinction between Jeans's mode and isotropic re-emission is important in considerations of angular momentum loss from the binary. Mass lost by the Jeans mode carries the specific angular momentum of the mass loser; isotropically re-emitted matter has the specific angular momentum of the accretor.

Wind hydrodynamics are ignored.

The fourth case considered is the intermediate mode, or mass loss to a ring. No mechanism for mass loss is hypothesised for this mode. The idea is simply that the ejecta has the high specific angular momentum characteristic of a circumbinary ring.

The differences among each of these modes is in the variation of the quantities $q$, $M_T$, and most importantly $L/\mu$, with mass loss. For example, given a $q = 0.25$ binary, mass lost into a circumbinary ring ($a_r > a$) removes angular momentum at least 25 times faster than mass lost by isotropic re-emission. This difference will have a great effect on the evolution of the orbit, as well as on the stability of the mass transfer.

**Table 1.** Names, brief description of, and dimensionless specific angular momentum of the modes of mass loss explored in this paper. Parameters $\alpha$, $\beta$, $\gamma$, $\delta$, $\epsilon$, and $A$ are defined in Eqs. (7), (8), (35), (37), and (14), respectively. The factor $A$ in the fast mode is typically unity

| Name of Mode | Type | $-\frac{\partial m_{mode}}{\partial m_2}$ | $\mu h_{loss}/L$ |
|---|---|---|---|
| Jeans/Fast | Isotropic wind | $\alpha$ | $\frac{A}{(1+q)^2}$ |
| — Isotropic Re-emission — | | $\beta$ | $\frac{q}{(1+q)^2}$ |
| Intermediate | Ring | $\delta$ | $\gamma$ |
| Slow | Accretion | $\epsilon$ | 0 |

In the following sections, formulae for the orbital evolution of a binary under different modes of mass loss are presented and integrated to give expressions for the change in orbital parameters with mass transfer. The different modes are summarised in Table (1).

Due to the formality of the following section and the cumbersome nature of the formulae derived, one should try to develop some kind of intuitition, and understanding of the results. The two sets of results (i.e.: one for a combination of winds, the other for ring formation) are examined in the limits of extreme mass ratios, compared to one another, and their differences reconciled in the first Appendix.

### *2.1. Unified wind model*

Consider first a model of mass loss which includes isotropic wind, isotropic re-emission, and accretion, in varying strengths. Conservative mass transfer, as well as pure forms of the two isotropic winds described above, can then be recovered as limiting cases by adjusting two parameters of this model:

$$\alpha = -\frac{\partial m_{wind}}{\partial m_2} , \tag{7}$$

$$\beta = -\frac{\partial m_{iso-r}}{\partial m_2} . \tag{8}$$

Here, $\partial m_{wind}$ is an infinitesimal mass of wind from star 2 (isotropic wind), and $\partial m_{iso-r}$ an infinitesimal mass of wind from star 1 (isotropic re-emission). Both amounts are expressed in terms of the differential mass $\partial m_2$, lost from star 2. A sign convention is chosen such that $\partial m_{star}$ is positive if the star's mass increases, and $\partial m_{flow}$ is positive if removing matter (from $m_2$). Given the above, one can write formulae for the variation of all the masses in the problem:

$$\epsilon_w \equiv 1 - \alpha - \beta \tag{9}$$

$$\partial \ln m_1 = -q\epsilon_w \, \partial \ln m_2 \tag{10}$$

$$\partial \ln M_T = \frac{q}{1+q}(\alpha + \beta) \, \partial \ln m_2 \tag{11}$$

$$\partial \ln q = (1 + \epsilon_w q) \, \partial \ln m_2 \tag{12}$$

$$\partial \ln \mu = \partial \ln m_2 - \frac{q}{1+q} \partial \ln q . \tag{13}$$

Neglecting accretion onto the stars from the ISM and mass currents originating directly from the accretor, all transferred mass comes from the mass donating star ($m_2$) and $\alpha$, $\beta$, and the accreted fraction $\epsilon_w$ all lie between 0 and 1, with the condition of mass conservation $\alpha+\beta+\epsilon_w = 1$, imposed by Eq. (9). For the remainder of this section, the subscript on $\epsilon_w$ will be eschewed.

If mass is lost isotropically from a nonrotating star, it carries no angular momentum in that star's rest frame. In the center of mass frame, orbital angular momentum $L$ will be removed at a rate $\dot{L} = h\,\dot{m}$, where $\dot{m}$ is the mass loss rate and $h$ the specific angular momentum of the orbit.

If a wind-emitting star is rotating, then it loses spin angular momentum $S$ at a rate $\dot{S} = R_W^2 \Omega_* \dot{m}$, where $\Omega_*$ is that star's rotation rate and $R_W^2$ the average of the square of the perpendicular radius at which the wind decouples from the star. Strongly magnetised stars with ionised winds will have a wind decoupling radius similar to their Alfvén radius, and spin angular momentum may be removed at a substantially enhanced rate.

The above consideration becomes important in the case of a tidally locked star, such as a Roche lobe filling red giant. In this case, if magnetic braking removes spin angular momentum from the star at some enhanced rate, that star will begin to spin asynchronously to the orbit and the companion will establish tides to enforce corotation. These tides are of the same form as those between the oceans and the Moon, which are forcing the length of the day to tend towards that of the month.

Strong spin-orbit coupling changes the evolution of orbital angular momentum in two ways. First, for a given orbital frequency, there is an extra store of angular momentum, due to the inertia of the star. Thus, for a given torque, $L$ evolves more slowly, by a factor $L/(L+S)$. The second is from the enhanced rate of loss of total angular momentum, due to the loss of spin angular momentum from the star. Extreme values of $R_W/R_*$ allow the timescale for loss of spin angular momentum to be much less than that for orbital angular momentum. Thus, the second effect will either compensate for or dominate over the first, and there will be an overall increase in the torque due to this wind.

This enhancement will be treated formally, by taking the angular momentum loss due to the fast mode to occur at a rate $A$ times greater than what would be obtained neglecting the effects of the finite sized companion.

Keeping the above discussion in mind, the angular momentum lost from the system, due to winds is as follows:

$$\partial L = (A\alpha h_2 + \beta h_1)\partial m_2 , \tag{14}$$

which can be simplified by substituting in expressions for the $h_i$:

$$h_i = L_i/m_i = (L/\mu)\frac{M_T - m_i}{M_T}\frac{\mu}{m_i} \tag{15}$$

$$h_1 = \frac{q^2}{1+q}\frac{L}{m_2} \tag{16}$$

$$h_2 = \frac{1}{1+q}\frac{L}{m_2} \tag{17}$$

$$\partial L = \frac{A\alpha + \beta q^2}{1+q}\frac{L}{m_2}\partial m_2 \tag{18}$$

$$\partial \ln L = \frac{A\alpha + \beta q^2}{1+q}\partial \ln m_2 \,. \tag{19}$$

So far, the equations have been completely general; $\alpha$, $\beta$, and $A$ may be any functions of the orbital elements and stellar properties. Restricting these functions to certain forms leads to simple integrable models of orbital evolution. If constant fractions of the transferred mass pass through each channel ($\alpha$, $\beta$ constant), then the masses are expressable as simple functions of the mass ratio $q$:

$$\frac{m_2}{m_{2,0}} = \left(\frac{q}{q_0}\right)\left(\frac{1+\epsilon q_0}{1+\epsilon q}\right) \tag{20}$$

$$\frac{m_1}{m_{1,0}} = \left(\frac{1+\epsilon q_0}{1+\epsilon q}\right) \tag{21}$$

$$\frac{M_T}{M_{T,0}} = \left(\frac{1+q}{1+q_0}\right)\left(\frac{1+\epsilon q_0}{1+\epsilon q}\right) \tag{22}$$

$$\frac{\mu}{\mu_0} = \left(\frac{q}{q_0}\right)\left(\frac{1+q_0}{1+q}\right)\left(\frac{1+\epsilon q_0}{1+\epsilon q}\right) \tag{23}$$

Furthermore, if the enhancement factor $A$ is also constant[2], then the angular momentum is an integrable function of $q$, as well:

$$\frac{L}{L_0} = \left(\frac{q}{q_0}\right)^{\mathscr{A}_w}\left(\frac{1+q_0}{1+q}\right)^{\mathscr{B}_w}\left(\frac{1+\epsilon q}{1+\epsilon q_0}\right)^{\mathscr{C}_w}, \tag{24}$$

where the exponents[3] are given by:

$$\mathscr{A}_w = A\alpha \,, \tag{25}$$

$$\mathscr{B}_w = \frac{A\alpha+\beta}{1-\epsilon} \,, \tag{26}$$

$$\mathscr{C}_w = \frac{A\alpha\epsilon}{1-\epsilon} + \frac{\beta}{\epsilon(1-\epsilon)} \,. \tag{27}$$

Finally, substitution of Eqs. (22), (23), and (24) into Eqs. (3) and (4) gives expressions for the evolution of the semimajor axis and orbital period in terms of the changing mass ratio $q$:

$$\frac{a}{a_0} = \left(\frac{q}{q_0}\right)^{2.\mathscr{A}_w-2}\left(\frac{1+q}{1+q_0}\right)^{1-2.\mathscr{B}_w}\left(\frac{1+\epsilon q}{1+\epsilon q_0}\right)^{3+2\mathscr{C}_w}, \tag{28}$$

$$\frac{P}{P_0} = \left(\frac{q}{q_0}\right)^{3.\mathscr{A}_w-3}\left(\frac{1+q}{1+q_0}\right)^{1-3.\mathscr{B}_w}\left(\frac{1+\epsilon q}{1+\epsilon q_0}\right)^{5+3\mathscr{C}_w}. \tag{29}$$

[2] This may not be the best approximation, if the orbit widens or narrows significantly and the torque is dominated by magnetic braking.

[3] There is no problem when the denominator $1-\epsilon \to 0$, as the numerator vanishes at the same rate. For $\mathscr{C}_w$, the power laws become exponentials in the absence of accretion ($\epsilon = 0$).

The derivatives of these functions may be evaluated either by logarithmic differentiation of the above expressions (Eqs. (28) and (29)), or by substitution of Eqs. (11), (12), (13), and (19) into Eqs. (5) and (6). Either way, the results are:

$$\frac{\partial \ln a}{\partial \ln q} = 2(.\mathscr{A}_w - 1) + (1 - 2.\mathscr{B}_w)\frac{q}{1+q} + (3 + 2\mathscr{C}_w)\frac{q}{1+\epsilon q} \,, \tag{30}$$

$$\frac{\partial \ln P}{\partial \ln q} = 3(.\mathscr{A}_w - 1) + (1 - 3.\mathscr{B}_w)\frac{q}{1+q} + (5 + 3\mathscr{C}_w)\frac{q}{1+\epsilon q} \,. \tag{31}$$

The reader should be convinced that the above equations are correct. First, and by fiat, they combine to give Kepler's law. Second, they reduce to the familiar conservative results:

$$\frac{a}{a_0} = \left(\frac{q_0}{q}\right)^2\left(\frac{1+q}{1+q_0}\right)^4, \tag{32}$$

$$\frac{P}{P_0} = \left(\frac{q_0}{q}\right)^3\left(\frac{1+q}{1+q_0}\right)^6, \tag{33}$$

in the $\epsilon = 1$ limit. Finally, and again by construction, the formulae are composable. Ratios such as $P/P_0$ are all of the functional form $f(q)/f(q_0)$, so if one forms e.g.: $(P_2/P_0) = (P_2/P_1)(P_1/P_0)$, the result is immediately independent of the arbitrarily chosen intermediate point $P_1 = P(q_1)$.

Note that the results for isotropic re-emission obtained by Bhattacharya & van den Heuvel (1991, Eq. (A.6)), and again by van den Heuvel (1994, Eq. (40)) are not composable, in the sense described above. The correct expression for $(a/a_0)$ in the case of isotropic re-emission may be obtained by setting $\alpha = 0$:

$$\frac{a}{a_0} = \left(\frac{q_0}{q}\right)^2\left(\frac{1+q_0}{1+q}\right)\left(\frac{1+(1-\beta)q}{1+(1-\beta)q_0}\right)^{5+\frac{2\beta}{1-\beta}}. \tag{34}$$

Also note that Eq. (A.7) of Bhattacharya & van den Heuvel (1991) should have its exponential in the numerator, as opposed to the denominator. In van den Heuvel (1994), Eq. (37) should read $\partial \ln J = \frac{\beta q^2}{1+q}\frac{\partial \ln q}{1+(1-\beta)q}$. In Eq. (38), an equals sign should replace the plus. (These corrections were also found by Tauris (1996)).

Thus, if there is mass loss from one star, with constant fractions of the mass going into isotropic winds from the donor and its companion, one can express the variation in the binary parameters, $M_T$, $a$, and $P$, in terms of their initial values, the initial and final values of the ratio of masses, and these mass fractions.

### 2.2. Formation of a coplanar ring

Now consider a model in which mass is transferred by accretion and ring formation, as described above. For concreteness, follow a standard prescription (cf: van den Heuvel (1994)) and take the ring's radius, $a_r$ to be a constant multiple $\gamma^2$ of the binary

semimajor axis. This effectively sets the angular momentum of the ring material, since for a light ring,

$$h_r = L_r/m_r = \sqrt{GM_T a_r} = \gamma L/\mu\,. \tag{35}$$

Formulae describing orbital evolution can be obtained acording to the prescription of the previous section. If a fraction $\delta$ of the mass lost from $m_2$ is used in the formation of a ring, then Eqs. (9) and (19) should be replaced as follows:

$$\begin{aligned} \epsilon_r &\equiv 1-\delta & (36)\\ \partial L &= \delta h_r\,\partial m_2 \\ &= \gamma\delta L/\mu\,\partial m_2 \\ &= \gamma\delta(1+q)L/m_2\,\partial m_2 & (37)\\ \partial \ln L &= \gamma\delta(1+q)\,\partial \ln m_2\,. & (38)\end{aligned}$$

Following the procedure used in Sect. (2.1), and with $\delta = 1$ ($\epsilon_r = 0$):

$$\begin{aligned} \frac{M_T}{M_{T,0}} &= \left(\frac{1+q}{1+q_0}\right)\,, & (39)\\ \frac{L}{L_0} &= \left(\frac{q}{q_0}\right)^{\gamma}\exp(\gamma(q-q_0))\,, & (40)\\ \frac{a}{a_0} &= \left(\frac{q}{q_0}\right)^{2(\gamma-1)}\left(\frac{1+q}{1+q_0}\right)\exp\left(2\gamma(q-q_0)\right)\,, & (41)\\ \frac{P}{P_0} &= \left(\frac{q}{q_0}\right)^{3(\gamma-1)}\left(\frac{1+q}{1+q_0}\right)\exp(3\gamma(q-q_0))\,. & (42)\end{aligned}$$

$$\begin{aligned} \frac{\partial \ln a}{\partial \ln q} &= 2\gamma(1+q)-2+\frac{q}{1+q}\,, & (43)\\ \frac{\partial \ln P}{\partial \ln q} &= 3\gamma(1+q)-3+\frac{q}{1+q}\,. & (44)\end{aligned}$$

Unless the ring is sufficiently wide ($a_r/a \gtrsim 2$), it will orbit in a rather uneven potential, with time-dependant tidal forces which are comparable to the central force. In such a potential, it would likely fragment, and could fall back upon the binary. Consequently, stability probably requires the ring to be at a radius of at least a few times $a$. A 'bare-minimum' for the ring radius is the radius of gyration of the outermost Lagrange point of the binary. This is between $a$ and $1.25a$, depending on the mass ratio of the binary (Pennington 1985). The ring should not sample the potential at this radius. For most of what follows, we will work with a slightly wider ring: $a_r/a = \gamma^2 = 2.25$ and $\delta = 1$.

## 3. Linear stability analysis of the mass transfer

Mass transfer will proceed on a timescale which depends critically on the changes in the radius of the donor star and that of its Roche lobe in response to the mass loss. The mass transfer might proceed on the timescale at which the mass transfer was initially driven (e.g.: nuclear, or orbital evolutionary), or at one of two much higher rates: dynamical and thermal.

If a star is perturbed by removal of mass, it will fall out of hydrostatic and thermal equilibria, which will be re-established on sound crossing (dynamical) and heat diffusion (Kelvin-Helmholtz, or thermal) timescales, respectively. As part of the process of returning to equilibrium, the star will either grow or shrink, first on the dynamical, and then on the (slower) thermal timescale. At the same time, the Roche lobe also grows or shrinks around the star in response to the mass loss. If after a transfer of a small amount of mass, the star's Roche lobe continues to enclose the star, then the mass transfer is stable, and proceeds on the original driving timescale. Otherwise, it is unstable and proceeds on the fastest unstable timescale.

In stability analysis, one starts with the equilibrium situation and examines the small perturbations about it. In this case, the question is whether or not a star is contained by its Roche lobe. Thus, one studies the behaviour of the quantity

$$\Delta\zeta = \frac{m}{R}\,\frac{\delta\Delta R}{\delta m}\,, \tag{45}$$

which is the (dimensionless) variation in the difference in radius between the star and its Roche lobe, in response to change in that star's mass. Here $\Delta R$ is the difference between the stellar radius $R_*$ and the volume-equivalent Roche radius $r_L$. The star responds to this loss of mass on two widely separated different timescales, so this analysis must be performed on both of these timescales.

The linear stability analysis then amounts to a comparison of the exponents in power-law fits of radius to mass, $R \sim m^{\zeta}$:

$$\begin{aligned} \zeta_s &\equiv \left.\frac{\partial \ln R_*}{\partial \ln m}\right|_s\,, & (46)\\ \zeta_{eq} &\equiv \left.\frac{\partial \ln R_*}{\partial \ln m}\right|_{eq}\,, & (47)\\ \zeta_L &\equiv \left.\frac{\partial \ln r_L}{\partial \ln m}\right|_{bin.evol.}\,, & (48)\end{aligned}$$

where $R_*$ and $m$ refer to the mass-losing, secondary star. Thus, $R_* = r_2$ and $m = m_2$. Stability requires that after mass loss ($\delta m_2 < 0$) the star is still contained by its Roche lobe. Assuming $\Delta R_2 = 0$ prior to mass loss, the stability condition then becomes $\delta\Delta R_2 < 0$, or $\zeta_L < (\zeta_s, \zeta_{eq})$. If this is not satisfied, then mass transfer runs to the fastest, unstable timescale.

Each of the exponents is evaluated in a manner consistent with the physical process involved. For $\zeta_s$, chemical abundance and entropy profiles are assumed constant and mass is removed from the outside of the star. For $\zeta_{eq}$, mass is still removed from the outside of the star, but the star is assumed to be in the thermal equilibrium state for the given chemical profile. In calculating $\zeta_L$, derivatives are to be taken along the assumed evolutionary path of the binary system.

In the following subsections these exponents are described a bit further and computed in the case of mass loss from a binary containing a neutron star and a Roche lobe-filling red giant.

Such systems are thought to be the progenitors of the wide orbit, millisecond pulsar, helium white dwarf binaries. They are interesting, both by themselves, and as a way of explaining the fossil data found in white dwarf – neutron star binaries. The problem has been treated by various authors, including Webbink et al. (1983), who evolved such systems in the case of conservative mass transfer from the red giant to the neutron star.

### *3.1. Adiabatic exponent: $\zeta_s$*

The adiabatic response of a star to mass loss has long been understood (see, for example, Webbink (1985) or Hjellming & Webbink (1987) for an overview), and on a simplistic level, is as follows. Stars with radiative envelopes (upper-main sequence stars) contract in response to mass loss, and stars with convective envelopes (lower-main sequence and Hayashi track stars) expand in response to mass loss. The physics is as follows.

A star with a radiative envelope has a positive entropy gradient near its surface. The density of the envelope material, if measured at a constant pressure, decreases as one samples the envelope at ever-increasing radii. Thus, upon loss of the outer portion of the envelope, the underlying material brought out of pressure equilibrium expands, without quite filling the region from which material was removed. The star contracts on its dynamical timescale, in response to mass loss.

A star with a convective envelope has a nearly constant entropy profile, so the preceding analysis does not apply. Instead, the adiabatic response of a star with a convective envelope is determined by the scalings among mass, radius, density, and pressure of the isentropic material. For most interesting cases, the star is both energetically bound, and expands in response to mass loss.

Given the above physical arguements, the standard explanation of mass-transfer stability is as follows. A radiative star contracts with mass loss and a convective star expands. If a convective star loses mass by Roche lobe overflow, it will expand with possible instability if the Roche lobe does not expand fast enough. If a Roche lobe-filling radiative star loses mass, it will shrink inside its lobe (detach) and the mass transfer will be stable.

This analysis "is of only a meagre and unsatisfactory kind" (Kelvin 1894), as it treats stellar structure in only the most simplistic way: convective vs. radiative envelope.

One can quantify the response of a convective star by adopting some analytic model for its structure, the simplest being an isentropic polytrope. This is a model in which the pressure $P$ and density $\rho$ vary as

$$P(r) = K\rho(r)^{1+1/n} \tag{49}$$

and the constituent gas has an adiabatic exponent related to the polytropic index through $\gamma = 1+1/n$. Other slightly more realistic cases include those with $\gamma \neq 1+1/n$, applicable to radiative stars; composite polytropes, with different polytropic indices for core and envelope; and centrally condensed polytropes, which are polytropes with a point mass at the center. These are all considered in a paper by Hjellming & Webbink (1987). We use the condensed polytropes, as they are simple, fairly realistic models of red giant stars, which tend in the limit of low envelope mass to (pointlike) proto-white dwarfs which are the secondaries in the low mass-binary pulsar systems.

What follows is a brief treatmant of standard and condensed polytropes, as applicable to the adiabatic response to mass loss.

Scaling arguements give $\zeta_s$ for standard polytropes. The pressure is an energy density and consequently scales as $GM^2R^{-4}$; density scales as $MR^{-3}$. The polytropic relation (Eq. (49)) immediately gives the scaling between $R$ and $M$. Since the material is isentropic, the variation of radius with mass loss is the same as that given by the radius-mass relation of stars along this sequence. Consequently, for polytropic stars of index $n$,

$$\zeta_s = \frac{n-1}{n-3}\,. \tag{50}$$

In particular, $\zeta_s = -1/3$ when $n = 3/2$ ($\gamma = 5/3$).[4]

The above approximation is fine towards the base of the red giant branch, where the helium core is only a small fraction of the star's mass. It becomes increasingly poor as the core makes up increasingly larger fractions of the star's mass, which happens when the star climbs the red giant branch or loses its envelope to RLOF. Mathematically speaking, the scaling law that lead to the formula for $\zeta_s$ is broken by the presence of another dimensionless variable, the core mass fraction.

A far better approximation to red giant structure, and only slightly more complex, is made by condensed polytropes, which model the helium core as a central point mass (see, e.g.: Hjellming & Webbink (1987)). Admittedly, this is a poor approximation, as concerns the core. However, the star's radius is much greater than that of the core, so this is a good first-order treatment. Furthermore, differences between this approximation and the actual structure occur primarily deep inside the star, while the star responds to mass loss primarily near the surface, where the fractional change in pressure is high. Overlap between the two effects is negligible.

Analysis of the condensed polytropes requires integrating the equation of stellar structure for isentropic matter (Lane-Emden equation), to get a function $R(S, M_c, M)$, and differentiating $R$ at constant specific entropy $S$ (adiabatic requirement) and core mass $M_c$ (no nuclear evolution over one sound crossing time). In general, the Lane-Emden equation is non-linear, and calculations must be performed numerically. The cases of $n = 0$ and $n = 1$ are linear and analytic. The case of $n = 1$ is presented below, as a nontrivial, analytic example, both for understanding, and because it can be used as a check of numeric calculations of $\zeta_s$.

The $n = 1$ Lane-Emden equation is (cf.: Clayton (1968)):

$$x^{-2}\frac{d}{dx}x^2\frac{d}{dx}\phi(x) = -\phi(x)\,. \tag{51}$$

[4] This formula also reproduces the two following results. The gas giant planets ($n = 1$) all have approximately the same radius. Massive white dwarfs ($n = 3$) are dynamically unstable.

Here, $x = r\sqrt{2\pi G/K} = r/\ell$ is the scaled radial coordinate and $\phi = \rho/\rho_c$ is the density, scaled to its central value[5]. The substitution $\phi(x) = x^{-1}u(x)$ allows solution by inspection:

$$\phi(x) = \frac{\sin(x)}{x} \qquad x \in [0, \pi]\,. \tag{52}$$

The polytropic radius is set by the position of the first root of $\phi$ and is therefore at $R = \pi\ell$. Similarly, $M = 4\pi^2\rho_c\ell^3$. Eq. (51) shows that the density ($\phi$) may be rescaled, without affecting the length scale, so $R$ is independent of $M$, and $\zeta_s = 0$.

Alternately, the $n = 1$ polytrope admits a length scale, $\ell$ which depends only on specific entropy, so the polytrope's radius is independent of the mass.

Generalising to condensed polytropes, Eq. (52) suggests the extension:

$$\phi(x) = \frac{\sin(x + x_0)}{x} \qquad x \in [0, \pi - x_0]\,. \tag{53}$$

For this model, the stellar radius, stellar mass, and core mass are

$$R = (\pi - x_0)R_0\,, \tag{54}$$

$$M = (\pi - x_0)M_0\,, \tag{55}$$

$$\begin{aligned} M_c &= M(x \to 0) \\ &= M_0 \sin(x_0)\,, \end{aligned} \tag{56}$$

for some $M_0$ and $R_0$. The core mass fraction

$$m = \frac{M_c}{M} = \frac{\sin(x_0)}{\pi - x_0} \tag{57}$$

is a monotonic function in $x_0$, and increases from 0 to 1 as $x_0$ increases from 0 to $\pi$. As the core mass fraction increases towards 1, the polytrope's radius decreases from $\pi R_0$ to 0, so the more condensed stars are also the smaller ones.

The adiabatic $R - M$ exponent $\zeta_s$ should be evaluated at constant core mass, as opposed to mass fraction. Thus, for condensed $n = 1$ polytropes,

$$\zeta_s = \frac{\sin(x_0)}{\sin(x_0) + (\pi - x_0)\cos(x_0)}\,, \tag{58}$$

where $x_0$ is chosen to solve Eq. (57). This solution matches that given by Eq. (50) when there is no core. Furthermore, $\zeta_s$ is an increasing function of the core mass fraction, which diverges, as $m = M_c/M$ tends towards unity. These are general features of the condensed polytropes, and hold for polytropic indices $n < 3$.

The procedure for calculating $\zeta_s$ is described in detail in Hjellming & Webbink (1987). Results for a variety of core mass fractions of $n = 3/2$ polytropes are given, both in Table 2 and graphically, in Figs. 1 and 3.

The function $\zeta_s(n = \frac{3}{2}; m)$ can be reasonably well fit by the function:

$$\zeta_{HW} = \frac{2}{3}\frac{m}{1-m} - \frac{1}{3} \tag{59}$$

[5] In general, $\rho = \rho_c\phi^n$.

**Table 2.** Adiabatic $R - M$ relation vs. core mass fraction $m_c$, as in Hjellming & Webbink (1987), Table 3. Columns two and four are the core-mass fraction and mass-radius exponent, respectively. The parameter $E$ in columns one and three is an alternate description of the degree of condensation of the polytrope, used by Hjellming and Webbink. The data presented here are in regions where the residuals of the fit formula Eq. (61) are in excess of 0.001

| $E$ | $m_c$ | $100\frac{dm_c}{dE}$ | $\zeta_s$ |
|---|---|---|---|
| 1.0 | 0.95144 | -4.7468 | 13.0293 |
| 2.0 | 0.90503 | -4.5372 | 6.31568 |
| 3.0 | 0.86066 | -4.3379 | 4.07567 |
| 4.0 | 0.81824 | -4.1484 | 2.95400 |
| 5.0 | 0.77766 | -3.9682 | 2.27964 |
| 6.0 | 0.73884 | -3.7967 | 1.82889 |
| 7.0 | 0.70170 | -3.6335 | 1.50588 |
| 32.0 | 0.13962 | -1.3079 | -0.11093 |
| 34.0 | 0.11442 | -1.2137 | -0.14849 |
| 36.0 | 0.09101 | -1.1279 | -0.18390 |
| 38.0 | 0.06925 | -1.0497 | -0.21759 |
| 40.0 | 0.04898 | -0.9785 | -0.24991 |

(Hjellming & Webbink 1987), and to better than a percent by either of the functions (in order of increasing accuracy):

$$\zeta_{SPH1} = \frac{2}{3}\left(\frac{m}{1-m}\right) - \frac{1}{3}\left(\frac{1-m}{1+2m}\right)\,, \tag{60}$$

$$\zeta_{SPH} = \zeta_{SPH1} - 0.03m + 0.2\left[\frac{m}{1+(1-m)^{-6}}\right]\,, \tag{61}$$

as shown graphically in Fig. 2.

### 3.2. Thermal equilibrium exponent: $\zeta_{eq}$

Analytic and numeric modeling of red giants have shown that the luminosity and radius depend almost entirely on the mass of the star's helium core (Refsdal & Weigert 1970; cf.: Verbunt (1993)). Since the core mass changes on the nuclear timescale, and we are interested in changes in the radius on the (much shorter) thermal timescale, the radius may be taken as fixed, giving $\zeta_{eq} = 0$.

### 3.3. Roche radius exponent: $\zeta_L$

Since the exponent $\zeta_L$ must be computed according to the evolution of the binary with mass transfer, it is sensitive to mass transfer mode, as are $M_T$, $a$, and $P$. The results for the various modes of nonconservative mass transfer are both interesting, and sometimes counterintuitive. It therefore makes sense to discuss them systematically and at some length.

We rewrite $\zeta_L$, in a form which depends explicitly on previously calculated quantities:

$$\begin{aligned} \zeta_L &= \frac{\partial \ln r_L}{\partial \ln m_2} \\ &= \frac{\partial \ln a}{\partial \ln m_2} + \frac{\partial \ln (r_L/a)}{\partial \ln q}\frac{\partial \ln q}{\partial \ln m_2}\,. \end{aligned} \tag{62}$$

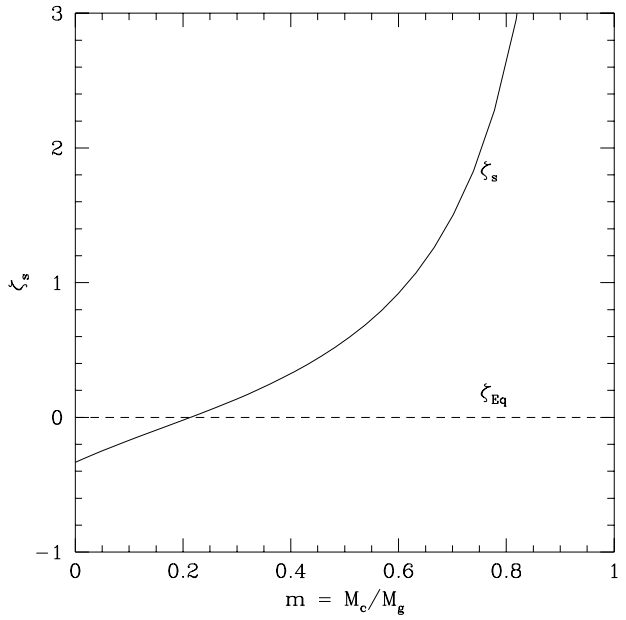


**Fig. 1.** Plot of $\zeta_s$ versus core mass fraction, of an isentropic, $n = 3/2$ red giant star. As the fraction of mass in the core grows, the star becomes less like a standard polytrope. Important to note is the crossing of the $\zeta_s$ and $\zeta_{eq}$ curves near $m_c/m_g = 0.2$

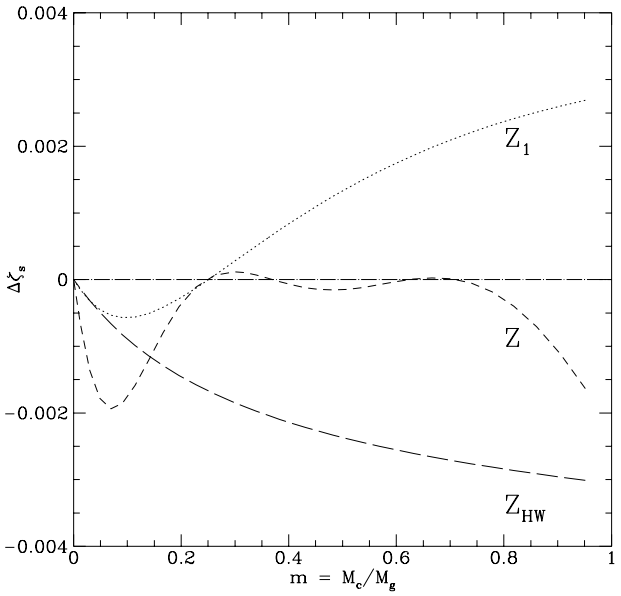


**Fig. 2.** Differences between various fit formulae and the function $\zeta_s(n = \frac{3}{2}; m)$. The labeled curves are as follows: $Z_{HW} = 0.01(\zeta_{HW} - \zeta_s)$, $Z_1 = 0.1(\zeta_{SPH1} - \zeta_s)$, and $Z = \zeta_{SPH} - \zeta_s$

The derivatives $\frac{\partial \ln a}{\partial \ln m_2}$ and $\frac{\partial \ln q}{\partial \ln m_2}$ appear in Sect. (2), both for the unified model, and for the ring; as well as in a tabulated form in Appendix A. All that remains is $\frac{\partial \ln (r_L/a)}{\partial \ln q}$, which will be calculated using Eggleton's (1983) formula for the volume-equivalent Roche radius:

$$r_L/a = \frac{0.49q^{2/3}}{0.6q^{2/3} + \ln(1+q^{1/3})}, \tag{63}$$

$$\frac{\partial \ln (r_L/a)}{\partial \ln q} = \frac{q^{1/3}}{3} \times \left( \frac{2}{q^{1/3}} - \frac{1.2q^{1/3} + \frac{1}{1+q^{1/3}}}{0.6q^{2/3} + \ln(1+q^{1/3})} \right). \tag{64}$$

To get an idea of how changing the mode of mass transfer effects stability, $\zeta_L$ has been plotted vs. $q$, for various models, in Figs. 4, 5, 6, and 7.

One notices several things in these graphs. Fig. 4 shows the extreme variation in $\zeta_L(q)$ with changes in mode of mass transfer. Each of the three curves 'ring', 'wind', and 'iso-r' differs greatly from the conservative case. At least as important is the extent to which they differ from one another, based only on the way in which these three modes account for the variation of angular momentum with mass loss. When angular momentum is lost at an enhanced rate, as when it is lost to a ring or a wind from the less massive star (direct wind, at low-$q$; isotropic re-emission at high-$q$), the orbit quickly shrinks in response to mass loss and $\zeta_L$ is high. By contrast, in the case of the isotropic wind in the high-$q$ limit, angular momentum is retained despite mass loss and the orbit stays wide, so $\zeta_L$ is lower than it is in the conservative case and the mass transfer is stabilised.

Second, Fig. 4 shows that ring formation leads to rather high $\zeta_L$, even for modest $\gamma^2 = a_r/a = 2.25$. The formation of a ring will usually lead to instability on the dynamical timescale ($\zeta_s < \zeta_{L,ring}$). The slower thermal timescale instability will occur only if the giant is rather evolved and has a high coremass fraction (with its high $\zeta_s$).

Delivery of mass to a ring would imply either a substantially larger, simultaneous flow of mass through the stabler of the two Jeans's channels, or else orbital decay, leading to dynamical timescale mass transfer.

Fig. 6 shows the variation of $\zeta_L$ due only to the differences between the isotropic wind and isotropic re-emission, in a family of curves with $\alpha + \beta = 0.8$. At $q = 1$, stability is passed from the mostly isotropic re-emission modes at low $q$ to mostly wind modes at high $q$. The $q = 1$ crossing of all these curves is an artifact of the model. Mass loss depends on the parameters in the combination $\alpha + \beta$. Angular momentum loss has a dependence $A\alpha + \beta q^2$. The two parameters $\alpha$ and $\beta$ are then equivalent at $q = \sqrt{A} = 1$.

For $q < 1$, mass transfer is stabilised by trading isotropic re-emission for wind, so families of $\alpha+\beta = const$ curves lie below their respective ($\beta = 0, \alpha$) curves in this region of the $q - \zeta_L$ graph. This becomes interesting when one examines the $\beta = 0$ curves, at high $\alpha$. For total wind strengths of less than about 0.85 and $q < 1$, $\zeta_L < 0$. Thus, for modest levels of accretion (at least $\sim 15\%$), with the remainder of mass transfer in winds, red giant - neutron star mass transfer is stable on the thermal timescale, so long as $q < 1$. If the donor red giant has a modest

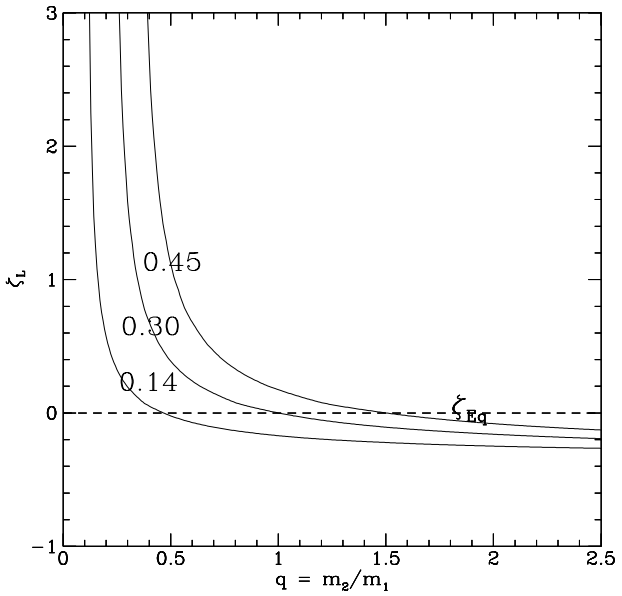


**Fig. 3.** Plots of $\zeta_s$ versus q, assuming a fiducial and constant $m_1 = 1.4M_\odot$. The three solid-line curves correspond, in ascending order, to core masses of 0.14, 0.30, and $0.45M_\odot$. Note that this figure is on the same scale as Figs. (4), et c., so that they may be overlaid

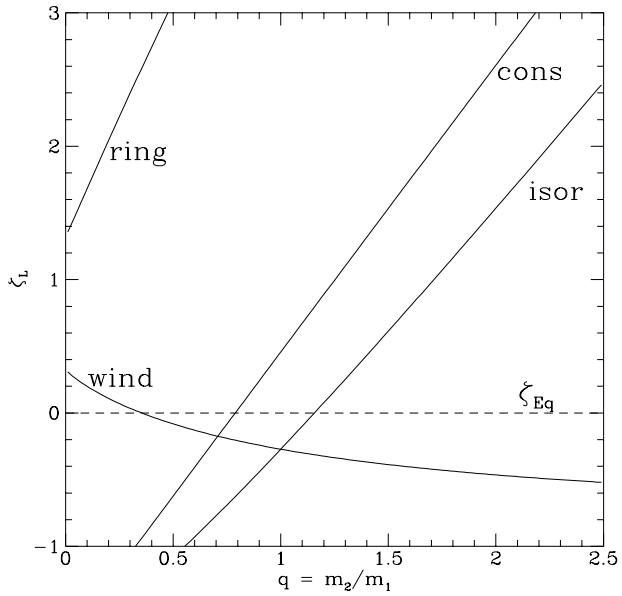


**Fig. 4.** $\zeta_L$ with all mass transfer through a single channel. For each curve, all mass from the donor star is transferred according to the indicated mode: conservative (cons); isotropic wind from donor star (wind); isotropic re-emission of matter, from vicinity of 'accreting' star (iso-r); and ring formation, with $\gamma = 1.5$. Since the unified model (winds+accretion) always has $0 \leq \alpha, \beta, \alpha + \beta \leq 1$, the $\zeta_L(q)$ curves labeled cons, wind, and iso-r also form an envelope around all curves in the unified model

mass core, so that $\zeta_s > 0$, then the process will be stable on he dynamical timescale, as well.

A family of curves with one wind of fixed strength and one wind of varying strength (as shown in Fig. 5, with $\beta = 0$, and variable $\alpha$), will also intersect at some value of $q$. It is easy to understand why this happens. For concreteness, take a constant-$\beta$ family of curves. Based on the linearity of the equations in $\alpha$ and $\beta$, $\zeta_L(q;\alpha,\beta) = f(q;\beta) + \alpha g(q)$, with some $f$ and $g$. If one evaluates $\zeta_L(q)$ at a root of $g(q)$, then the result is independent of $\alpha$.

Notice in each case, intersections of various unified wind model $\zeta_L(q)$ curves occur at $q = O(1)$. One can understand this, in the framework of the arguments of Sect. (A). Depending on which side of $q = 1$ one lies, either $m_1$ or $m_2$ has the majority of the angular momentum. When $q < 1$, angular momentum will be lost predominantly by the isotropic wind and $\zeta_L$ will be high. When $q > 1$, angular momentum losses will be modest and $\zeta_L$ low. The situation is reversed for isotropic re-emission. The two curves form a figure-X on the $q - \zeta_L$ diagram and must cross when neither $q$, nor $1/q$ is too great; that is, near $q = 1$.

## 4. An example: mass transfer in red giant – neutron star binaries

Consider a binary system composed of a neutron star and a less evolved star. The less evolved star burns fuel, expanding and chemically evolving. If the binary orbital period is sufficiently short, the evolving star will eventually fill its Roche lobe and transfer mass to its companion. We now consider this problem, in the case where mass transfer starts while the donor is on the red giant branch (The so-called case B. See e.g.: Iben & Tutukov 1985.).

The global properties of an isolated star are functions of the stellar mass and time from zero age main sequence. Alternately, red giant structure can be parameterised by total mass and core mass. Detailed models show that the dependence on total mass is weak, so the radius and luminosity are nearly functions of the core mass, only. We use the fit formulae by Webbink (1975), who writes:

$$r = R_\odot \exp(\sum c_i y^i) , \tag{65}$$

$$L = L_\odot \exp(\sum a_i y^i) \tag{66}$$

$$= X\varepsilon_{CNO}\dot{m}_c . \tag{67}$$

Here $y = \ln(4m_c/M_\odot)$, and the parameters $a_i$, and $c_i$ are the result of fits to the red giant models (See Table 3.). Eq. (67) assumes that the red giant's luminosity comes solely from shell hydrogen burning by the CNO cycle, which produces energy at a rate $\varepsilon_{CNO} = 5.987 \cdot 10^{18}$erg g$^{-1}$ (Webbink et al. 1983).

The red giant eventually fills its Roche lobe, transferring mass to the other star. If mass transfer is stable, according to the criteria in Sect. 3, then one can manipulate the time derivatives of $r$ and $r_L$ to solve for the rate of mass loss from the giant. The stellar and Roche radii vary as:

$$\dot{r} = \left.\frac{\partial r}{\partial t}\right|_{m_g} + r\,\zeta_{eq}\frac{\dot{m}_g}{m_g} , \tag{68}$$

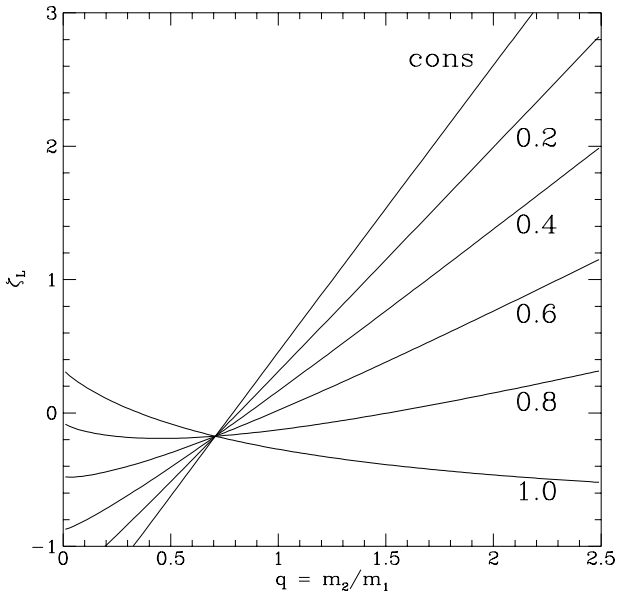


**Fig. 5.** This illustrates the effect of an increasing fraction of the mass lost from the donor star ($m_2$) into a fast wind from that star. Solid lines correspond to $\alpha \in 0.0(0.2)1.0$ from top to bottom on the graph's right side; $\alpha = 0$ corresponds to conservative mass transfer. Note that at $q \sim 0.72$, $\zeta_L(\beta = 0)$ is independent of $q$

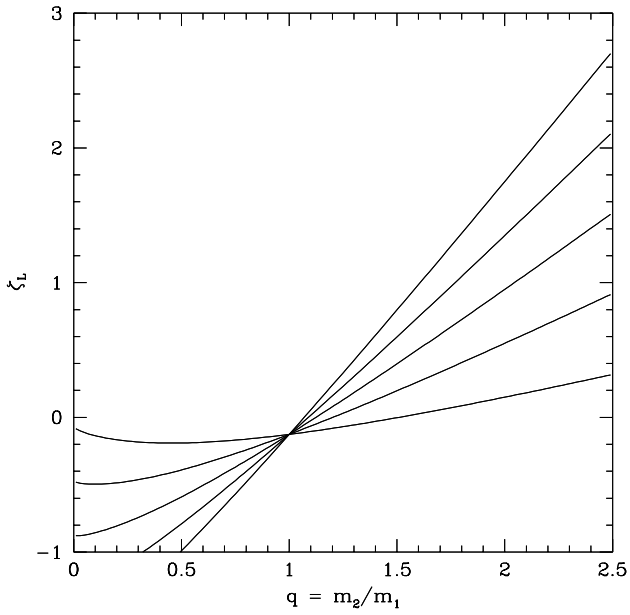


**Fig. 6.** The change in $\zeta_L(q)$ for all mass lost to isotropic winds, with varying fractions in isotropic wind and isotropically re-emiiited wind. From top to bottom on the right side, the solid curves are for $(\alpha, \beta)$ of $(0.0, 0.8)$, $(0.2, 0.6)$, $(0.4, 0.4)$, $(0.6, 0.2)$, and $(0.8, 0.0)$. Note that all curves cross at $q = 1$. Any set of curves $\alpha + \beta = const.$ will intersect at $q = 1$, as at this point, $\alpha$ and $\beta$ have the same coefficients in $\zeta_L$

$$\dot{r}_L = \left.\frac{\partial r_L}{\partial t}\right|_{m_g} + r_L \zeta_L \frac{\dot{m}_g}{m_g} . \tag{69}$$

So long as the star remains in contact with its Roche lobe,

$$\frac{\dot{m}_g}{m_g} = \frac{1}{\zeta_L - \zeta_{eq}} \left( \frac{\partial \ln r}{\partial t} - \frac{\partial \ln r_L}{\partial t} \right)_{m_g} , \tag{70}$$

$$\frac{\dot{r}}{r} = \frac{\dot{r}_L}{r_L} ,$$

$$\frac{\dot{r}}{r} = \left.\frac{\partial r}{\partial t}\right|_{m_g} \left( \frac{\zeta_L}{\zeta_L - \zeta_{eq}} \right) + \left.\frac{\partial r_L}{\partial t}\right|_{m_g} \left( \frac{\zeta_{eq}}{\zeta_L - \zeta_{eq}} \right) . \tag{71}$$

The first term in Eq. (69) takes into account changes in the Roche radius not due to mass transfer, such as tidal locking of a diffuse star or orbital decay by gravitational wave radiation. For the models considered here, the Roche lobe evolves only due to mass transfer. Eqs. (69), (70), and (71) then reduce to the two equations:

$$\dot{r}_L = r_L \zeta_L \frac{\dot{m}_g}{m_g} . \tag{72}$$

$$\frac{\dot{m}_g}{m_g} = \frac{1}{\zeta_L - \zeta_{eq}} \left( \frac{\partial \ln r}{\partial t} \right)_{m_g} . \tag{73}$$

The additional relation:

$$\frac{\partial \ln r}{\partial t} = \frac{\partial \ln r}{\partial \ln m_c} \frac{\partial \ln m_c}{\partial t} \tag{74}$$

is a consequence of the star being a red giant.

**Table 3.** Parameters fitted to a series of red giant models, both for Pop I ($Z = 0.02$, $X = 0.7$) and Pop II ($Z = 10^{-4}$, $X = 0.7$). Data are transcribed from Webbink et al. (1983), and are applicable over the ranges $y \in (-0.4, 0.6)$ and $y \in (-0.2, 0.4)$ for Pop I and Pop II, respectively. Pop I figures due to Webbink (1975); Pop II from Sweigart & Gross (1978)

| Z | $a_0$ | $a_1$ | $a_2$ | $a_3$ |
|---|---|---|---|---|
| 0.02 | 3.50 | 8.11 | -0.61 | -2.13 |
| $10^{-4}$ | 3.27 | 5.15 | 4.03 | -7.06 |

| Z | $c_0$ | $c_1$ | $c_2$ | $c_3$ |
|---|---|---|---|---|
| 0.02 | 2.53 | 5.10 | -0.05 | -1.71 |
| $10^{-4}$ | 2.02 | 2.94 | 2.39 | -3.89 |

The equations for the evolution of the core mass, red giant mass, neutron star mass, orbital period, and semimajor axis (obtainable from Eqs. (67), (73), (74), (11), (31), and (30)), form a complete system of first order differential equations, governing the evolution of the red giant and the binary. The core mass grows, as burned hydrogen is added from above. This causes the star's radius to increase, which forces mass transfer, increasing $a$ and $P$, at $r_L = r_g$.

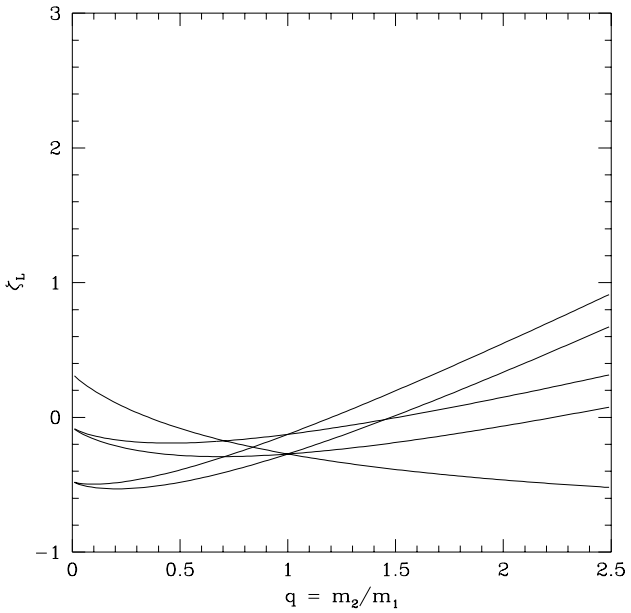


**Fig. 7.** $\zeta_L$ for various $\alpha$ and $\beta$, so that most transferred mass is ejected as winds. From top to bottom on the right side, the solid curves are for $(\alpha, \beta)$ of $(0.6, 0.2)$, $(0.6, 0.4)$, $(0.8, 0.0)$, $(0.8, 0.2)$, and $(1.0, 0.0)$

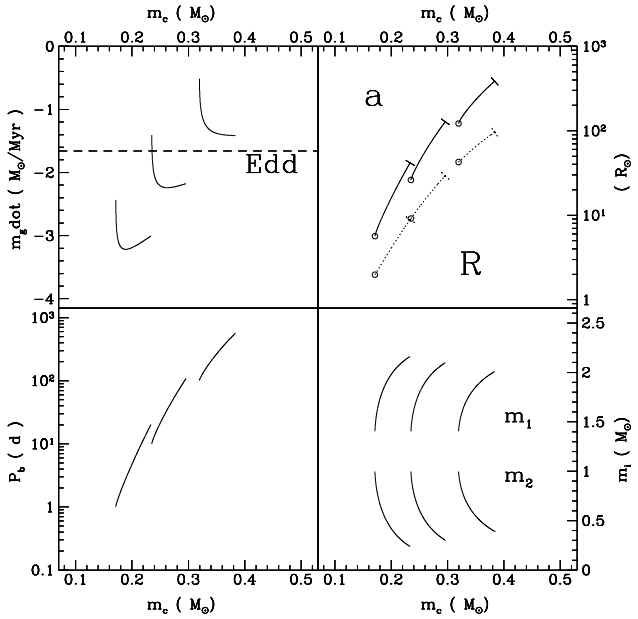


**Fig. 8.** This figure shows conservative evolution in three different red giant neutron star binaries, initial with $m_X = 1.4M_\odot$, $m_g = 1.0M_\odot$, and $P_i = 1, 10, 100$ days. Red giant coremass increases monotonically as the system evolves and has been chosen as the independent variable. The lower right hand panel shows the evolution of the two stars' masses, with increasing $m_c(t)$; the neutron star's mass ($m_1$) increases, with complementary a decrease in the mass of the giant ($m_2$). Orbital period evolution is shown in the lower left hand panel. The mass transfer decreases the mass of the lower mass star, and consequently widens the orbit ($P$ increases, at constant $M_T$ and $L$; Eq. (29)). The upper right hand panel shows the evolution of semimajor axis (upper, solid curves) and red giant Roche radius (lower, dashed curves). The low and high coremass ends of each segment in this panel are indicated by a circle and crossbar, for clarity. While transferring mass, the red giant fills its Roche lobe, so the dashed segments shown here are consistent with the giant's coremass radius relation (Eq. (65)). Finally, the upper left hand panel shows the red giant mass loss rate. The dotted line labeled 'Edd' is the Eddington limit accretion rate of the neutron star ($\dot{m}_X = 4\pi R_X c/\kappa_{Th}$, with an assumed neutron star radius $R_X = 10\,km$ and $X_H = 0.70$. General relativistic effects and the variation of neutron star mass and radius with accretion have been ignored.). At high coremasses, where the red giant's evolution is rapid, the mass loss rate can be far in excess of the neutron star's Eddington rate, implying that mass transfer is not always conservative

### *4.1. The code*

The program used to generate the numbers presented here follows the prescription outlined by Webbink et al. 1983, in the treatment of initial values, numeric integration of the evolution, and prescription for termination of mass transfer. The solar mass, radius, and luminosity are taken from Stix (1991).

Initial values were provided for the masses of the neutron star, the red giant, and its core at the start of the contact phase (red giant filling its Roche lobe): $m_X$, $m_g$, and $m_c$, respectively, as well as for the parameters ($\alpha$, $\beta$, $\gamma$...) of the mass transfer model. A tidally-locked system was assumed and spin angular momentum of the stars neglected. The program then solved for the orbital period $P$ and separation, $a$, using relations (2), (63), and (65).

Integration of Eqs. (10), (6), (67), and (73) was performed numerically by a fourth-order Runge-Kutta scheme (cf.: Press et al. 1986) with time steps limited by $\Delta m_g \leq 0.003 m_g$, $\Delta m_c \leq 0.001 m_c$, and $\Delta m_e \leq 0.003 m_e$. The first two criteria are those used by WRS; the last was added to this code, to insure that care is taken when the envelope mass, $m_e$, becomes small toward the end of the integration.

Detailed numeric calculations (Taam 1983) show that a red giant cannot support its envelope if $m_e/m_g < 0.02$. The code described here follows that of WRS and terminates mass transfer at this point.

An overdetermined system of $m_c$, $m_g$, $m_X$, and $P$ was integrated numerically by the code, allowing for consistancy checks of the program. Tests performed at the end of the evolution included tests of Kepler's law (Eq. (2)), angular momentum evolution (Eq. (29) or (42)), and a check of the semi-detatched requirement $r_2 = r_L = a\cdot(r_L/a)$. Plots of various quantities versus red giant core mass show the evolutionary histories of binary systems, in Figs. 8, 9, and 10. Population I stars were used in all calculations (see Table 3; $Z = 0.02$).

Another interesting case of mass transfer is isotropic re-emission at the minimum level necessary to ensure Eddington limited accretion:

$$\beta = \max(0, \dot{m}_g/\dot{m}_{X,Edd} - 1)\,. \tag{75}$$

Re-emission would presumably be in the form of propeller ejecta (Ghosh & Lamb (1978) or a bipolar outflow, such as the

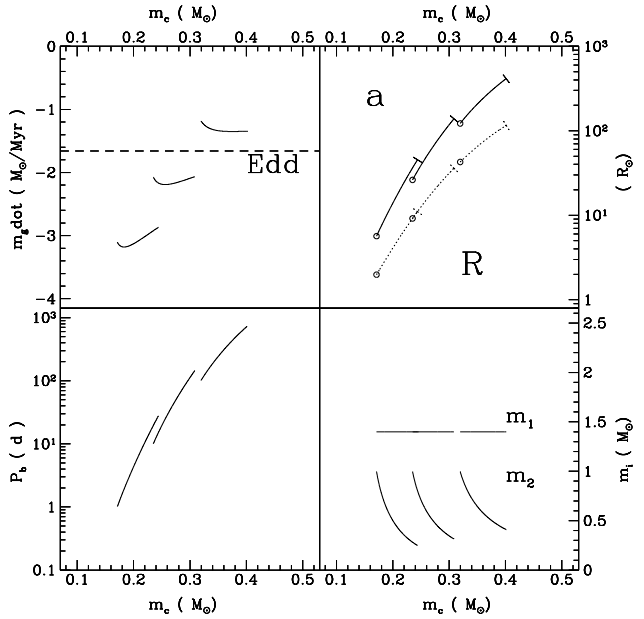


**Fig. 9.** Mass transfer by isotropic re-emission ($\alpha$ = 0, $\beta$ = 1); details as in Fig. 8

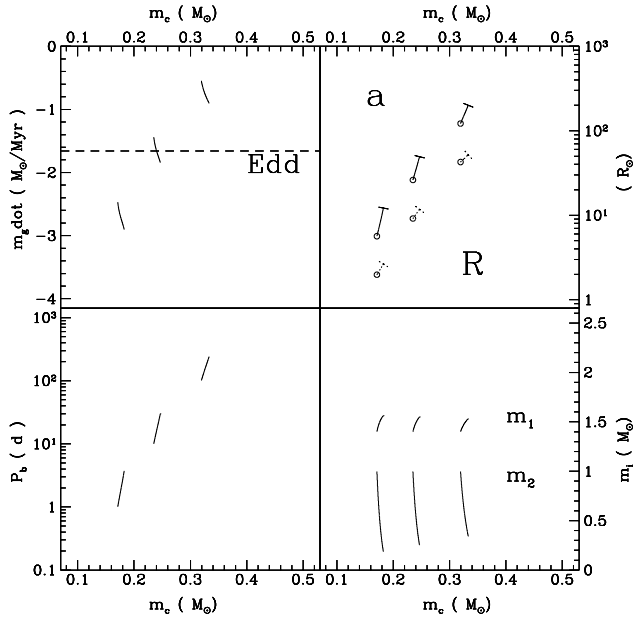


**Fig. 10.** Mass transfer by a combination of accretion and wind ($\alpha$ = 0.8, $\beta$ = 0). The pure wind gives similar results for initial periods of 10 and 100 days, but leads to instability for short initial periods. This instability in low core mass systems is easily understood, since shorter period systems can evolve towards lower mass ratio systems, where $\zeta_L(\alpha = 1, \beta = 0) > \zeta_{eq}$. See also Fig. 8 for details

jets seen in the galactic superluminal sources. The evoution of a binary, subject to this constraint, is shown in Fig. 11. Comparing Fig. 11 with Figs. 8 and 9, one sees that the low core mass systems, with their corresponding low mass transfer rates, mimic conservative systems. The faster evolving systems behave more like systems with pure isotropic re-emission.

Almost all ring-forming systems are unstable to thermal and/or dynamical timescale runaway of mass transfer, and are not displayed.

## 5. Conclusion

Previous works in the field of mass transfer in close binaries usually centered on conservative mass transfer, even when observation directs us to consider mass loss from the system, as is the case with white dwarf neutron star binaries. If these systems form from mass transfer in red giant neutron star systems, then one must find a way to start with a secondary star sufficiently massive to evolve off the main sequence in a Hubble time, ($m_2 > 1M_\odot$), in a binary with a $m_X > 1.3M_\odot$ neutron star and reduce the secondary's mass by $\approx 0.6M_\odot$, while keeping the neutron star below $\sim 1.45M_\odot$. To do this, some 3/4 of the mass from the secondary must be ejected from the system. Results here indicate that it is possible to remove this much mass in winds, while maintaining stable mass transfer on the nuclear timescale.

For the most part, nonconservative mass transfer, in which mass is lost in fast winds, mimics the conservative case. For the typical initial mass ratios ($q \approx 0.7$), $\zeta_L$ ranges from about -0.7 to -0.2. The rate of mass transfer is given by Eq. (73), and is lowest at the start of mass transfer, when $m_c$ is low. The total time is therefore set almost entirely by $m_c(0)$ and $\zeta_L(0)$, and so differs by maybe a factor of 3, over all possible wind models.

It is worth repeating that changes in $M_T$ arising from nonconservative evolution do not alter the relationship between white dwarf mass and binary period by more than a couple of percent. This is true, by the following arguement. The final red giant and core masses differ only at the few percent level. Approximately, then, the red giant mass sets the red giant radius and therefore the Roche radius. In the (low $q$) approximation used by Paczyński (1971), orbital period is a function of $r_L$ and $m_2$, only. $P$ vs. $m_c$ is a function of the final state, alone. Using Eggleton's formula instead of Paczyński's introduces only a very weak dependence on the mass of the other (neutron) star. In the end, the theoretical motivation for the existence of a $P - m_c$ relation is significantly more solid than, say, our knowledge of the red giant $R - m_c$ relation, on which the exact $P - m_c$ curve depends.

The exact mode of mass transfer will effect $P/P_0$, as is evident from Eq. (29). This could be important, in statistical studies of white dwarf neutron star binaries, and trying to predict the distribution of $P$ from the initial mass function, and distribution of initial orbital periods. This is dependent, of course, on the development of a quantitative understanding of the common envelope phase.

Finally, and probably the most useful thing, is that if one assumes only accretion and wind-like mass transfer, then most binaries in which mass is transferred from the less massive star are stable on both dynamical and thermal timescales. If the mass

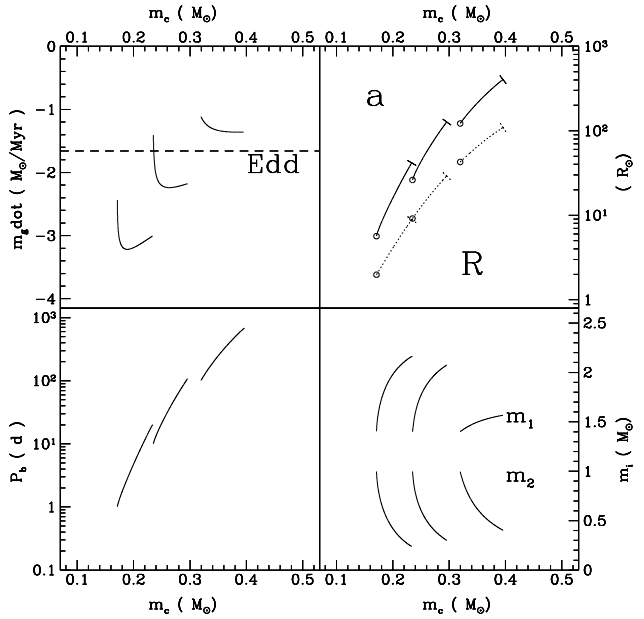


**Fig. 11.** Mass transfer with isotropic re-emission only so strong as to insure $\dot{m}_X \leq \dot{m}_{X,Edd}$. For details, see Fig. 8

donor has a radiative envelope (not treated here), it will shrink in response to mass loss, and lose mass in a stable way. If the donor has a convective envelope, a modestly sized core will stabilize it sufficiently to prevent mass loss on the dynamical timescale. Only if one has a very low mass (or no) core, will the mass transfer be unstable on the dynamical timescale, and then, only for $\alpha \to 1$. High values of $\alpha$, and low core mass in a convective star may lead to instability on the thermal timescale, if the mass ratio, $q$ is sufficiently low (see Fig. 5).

*Acknowledgements.* This work was supported by NSF grant AST93-15455 and NASA grant NAG5-2756.

## Appendix A: mass transfer models with extreme mass ratios

The results of Sects. 2.1 and 2.2 are examined here in the limiting cases of $q$ tending toward zero and infinity, to explore the relations between the different modes, and the connections to well-known toy models. This is done to develop an intuition which may be used in comparing the stability of mass transfer by the various modes.

In considering extreme values of the mass ratio, one makes the reduced mass approximation, regarding all the mass as residing in one star of fixed position and all the angular momentum in the other, orbiting star. Errors are only of order $q$ (or $1/q$, if this is small). One might keep the Solar System in mind as a concrete example. The Sun has all the mass, and the total angular momentum is well approximated by Jupiter's orbital angular momentum. The total mass $M_T \sim M_\odot$ and the reduced mass $\mu \sim M_J$, with fractional errors $\sim M_J/M_\odot \sim 10^{-3}$.

Retention of the factors $A$ (Eqs. (19), et seq. of Sect. 2.1) and $\delta$ (Eq. (38), of Sect. 2.2) allow for broader comparisons between the two models. Formulae appropriate to the two extreme limits are in Table 4. Columns 2 and 3 pertain to the wind models; 4 and 5 to ring models.

**Table 4.** Formulae describing orbital evolution in the limits of extreme mass ratios, $q = m_2/m_1 \ll 1$ and $q \gg 1$

| | Winds | | Ring | |
|---|---|---|---|---|
| | $q \to 0$ | $q \to \infty$ | $q \to 0$ | $q \to \infty$ |
| $\frac{\partial \ln q}{\partial \ln m_2}$ | $1$ | $q(1-\alpha-\beta)$ | $1$ | $q(1-\delta)$ |
| $\frac{\partial \ln M_T}{\partial \ln m_2}$ | $0$ | $\alpha+\beta$ | $0$ | $\delta$ |
| $\frac{\partial \ln L/\mu}{\partial \ln m_2}$ | $A\alpha-1$ | $q(1-\alpha)$ | $\gamma\delta-1$ | $q(\gamma\delta+(1-\delta))$ |
| $\frac{\partial \ln P}{\partial \ln q}$ | $3(A\alpha-1)$ | $3\frac{1-\alpha}{1-\alpha-\beta}$ | $3(\gamma\delta-1)$ | $3\frac{\gamma\delta+(1-\delta)}{1-\delta}$ |
| $\frac{\partial \ln a}{\partial \ln q}$ | $2(A\alpha-1)$ | $2\frac{1-\alpha}{1-\alpha-\beta}$ | $2(\gamma\delta-1)$ | $2\frac{\gamma\delta+(1-\delta)}{1-\delta}$ |
| $\frac{q}{q_0}$ | $\frac{m_2}{m_{2,0}}$ | $\frac{M_{T,0}}{M_T}$ | $\frac{m_2}{m_{2,0}}$ | $\frac{M_{T,0}}{M_T}$ |
| $\frac{M_T}{M_{T,0}}$ | $1$ | $\frac{q_0}{q}$ | $1$ | $\frac{q_0}{q}$ |
| $\frac{(L/\mu)}{(L/\mu)_0}$ | $\left(\frac{q}{q_0}\right)^{A\alpha-1}$ | $\left(\frac{q}{q_0}\right)^{\frac{A\alpha-1}{1-\alpha-\beta}}$ | $\left(\frac{q}{q_0}\right)^{\gamma\delta-1}$ | $\left(\frac{q}{q_0}\right)^{\frac{\gamma\delta+(1-\delta)}{1-\delta}}$ |
| $\frac{P}{P_0}$ | | $\left(\frac{(L/\mu)}{(L/\mu)_0}\right)^3$ | | |
| $\frac{a}{a_0}$ | | $\left(\frac{(L/\mu)}{(L/\mu)_0}\right)^2$ | | |

It is now straightforward to compare the two models of mass transfer and loss in the extreme limits where they should be equivalent. Comparisons will be made first in the limit where the donor is a test-mass, where the unified and ring models correspond exactly. Second will be a treatment of the opposite limit, where the two models give different but reconcilable results.

First, the wind and ring models are equivalent in the $q = 0$ limit, upon identification of $\alpha$ with $\delta$ and $A$ with $\gamma$[6]. This symmetry is not difficult to understand. In the $q = 0$ limit, only the direct isotropic wind and ring remove angular momentum. In this case, isotropic re-emission is an isotropic wind from a stationary source, and accretion is always conservative of both mass and angular momentum. In each torquing case (direct wind and ring), the ejected mass removes specific angular momentum at an enhanced rate — $A$ in the winds model, $\gamma$ in the ring model. Thus, it makes sense that wherever $A$ and $\gamma$ appear in the equations, they are in the products $A\alpha$ and $\gamma\delta$, the rate of angular momentum loss per unit mass lost from $m_2$.

More interesting is that, in the strict $q = 0$ limit, the parameters $\alpha$ and $\delta$ are found only in the combinations $A\alpha$ and $\gamma\delta$.

[6] Actually, one must only identify the products of mass fraction lost and relative specific angular momenta: $A\alpha$ and $\gamma\delta$.

The independence from other combinations of parameters can be understood by examining the ratio

$$\eta = \left.\frac{\partial \ln M_T}{\partial \ln (L/\mu)}\right|_{ev}, \tag{A1}$$

which tells the relative importance of angular momentum and mass losses in the orbit's evolution. For small donor mass, $\eta$ is small and mass loss without angular momentum loss is unimportant. The strict mass loss term will be important only when the coefficient of the $\partial \ln (L/\mu)$ term, $A\alpha - 1$ or $\gamma\delta - 1$, is of order $q$ or less. This happens, for example, in the Jeans' mode of mass loss ($q \ll 1$, $A = \alpha = 1$), discussed below.

Even neglecting the questions of stability important to tidally induced mass transfer, the situation is different when the mass–losing star has all the mass and almost no angular momentum. In this case, both mass and angular momentum loss are important. Since the more massive body is the mass donor, a non-negligible fraction of the total mass of the system may be ejected. Furthermore, the angular momentum per reduced mass changes via isotropic re-emission and ring formation. Therefore, both mass and angular momentum loss play a rôle in the dynamics. A measure of relative importance is $\eta$, which in the limit of large $q$, goes as $1/q$. Again, in the case of extreme mass ratios, changes in $L/\mu$ dominate the course of evolution. As before, there are times when the coefficient of the $\partial \ln (L/\mu)$ term, $1 - \alpha$ or $\gamma\delta + (1 - \delta)$, is of order $q$, or less. In this case, the above arguments fail and the strict mass loss term $\partial \ln M_T$ must be included.

The evolution of the angular momentum per reduced mass shows a significant difference the winds and ring models in their $q \gg 1$ limit. In the wind case, one may write $q(1 - \alpha) = q(1 - \alpha - \beta) + q\beta$. The first part is the fractional rate of increase of $\mu$, with loss of mass from the donor star. The second is the rate at which angular momentum is lost from the system, by isotropic re-emission. Since $q \gg 1$, the mass losing star is nearly stationary and mass lost in a direct wind removes no angular momentum.

The ring + accretion case is slightly different, but may be interpreted similarly. The term $q(1-\delta)$ replaces $q(1-\alpha-\beta)$ as the fraction of mass accreted onto the first star; i.e.: $\partial \ln \mu / \partial \ln m_2$. The term $q\beta$ is replaced by $q\gamma\delta$, as the rate of loss of angular momentum. Although the donor star is stationary in this $q \gg 1$ ring case, angular momentum is still lost. This is due to the particular construction of the ring model, in which the angular momentum removed is proportional to the system's $L/\mu$, not to the specific angular momentum of either body. Thus, in the ring model, even as $h_2$ tends towards zero with increasing $q$, ejected mass will carry away angular momentum. This is the final *caveat*: the ring model is just a mechanism for the rapid removal of angular momentum from a binary system, and one should keep this in mind, particularly when $q \gg 1$.

One might also notice for both models, that if angular momentum loss is not overly efficient ($A$ and $\gamma$ not too much greater than 1), then mass loss from the test mass widens the orbit and mass loss from the more massive star shrinks the orbit, just like in conservative mass transfer. Also, $\eta$ is not everywhere small. In particular, when $q$ is of order unity, $\eta$ is also and the $\partial \ln M_T$ term becomes as important as $\partial \ln (L/\mu)$ in the equations of motion.

### *5.1. Jeans's modes*

Often, one talks of the Jeans's mode of mass loss from a binary, in which there is a fast, sperically symmetric loss of mass. The Jeans' mode has two limits. One is a catastrophic and instantaneous loss of mass, as in a supernova event (see van den Heuvel (1994), for a discussion). In this case, if the orbit is initially circular and more than half the total mass is lost in the explosion, the system unbinds. This can be explained by the energetics. Initially, the system is virialised with $< T >= -1/2 < V >$. The loss of mass does not change the orbital velocities, so the kinetic energy per unit mass remains the same. The potential energy per unit mass is proportional to the total mass, so if more than half the mass is lost, $E = T + V > 0$ and the orbit is unbound. A more detailed analysis may be done, and will give ratios of initial to final orbital periods and semi-major axes, for given initial to final mass ratios (Blaauw (1961); Flannery & van den Heuvel (1975)).

The equations in this paper will not give the 'standard' Jeans solution and unbound orbits. Unbinding the orbit from elliptical to hyperbolic requires $e > 1$, where $e = 0$ has been assumed from the outset. The argument used in the preceding paragraph seemingly necessitates the unbinding of the orbit with sufficient mass loss, but it is not applicable here, as it also assumes a conservation of mechanical energy. Mechanical energy is not conserved in the above calculations (Sect. (2.1), for example), as the presence of dissipative forces to damp $e$ to 0 have been assumed.

The other limit of Jeans's mode is mass loss by a fast wind, on a timescale slow compared to the orbital period. In this case, there is no preferred orientation for the Runge-Lenz vector (direction of semimajor axis in an eccentric orbit), and the orbit remains circular throughout the mass loss, with $M_T a = const.$ This is the limit of the Jeans mode which our calculations reproduce. Jeans's mode is an example of a degenerate case (mentioned above; here, $A\alpha = 1$), where $\partial \ln (L/\mu) = 0$. In this case, one may simply apply Eq. (3), and see that $GM_T a = (L/\mu)^2 = const.$

## Appendix B: extensions to models considered above

In the interest of completeness, a five-parameter model of mass transfer, combining winds from both stars, ring formation, and accretion is presented. The treatment in Sects. 2 and 3.3 is followed. Modifications necessary for inclusion of other forms of angular momentum loss, such as $\dot{L}_{GR}$, due to gravitational radiation reaction, are also discussed.

Construction of this model is straightforward, and results from the inclusion of the various sinks of mass and angular momentum, due to various processes. The nonconservative part of each model makes its own contribution to the logarithmic

derivatives of $M_T$ and $L$:

$$\epsilon \equiv 1-\alpha-\beta-\delta\ , \tag{B1}$$

$$\partial \ln M_T = (1-\epsilon)\frac{q}{1+q}\,\partial \ln m_2\ , \tag{B2}$$

$$\partial \ln L = \left(\frac{A\alpha+\beta q^2}{1+q}+\gamma\delta(1+q)\right)\partial \ln m_2\ , \tag{B3}$$

where each of the variables retains its old meaning. Replacing the old definition of $\epsilon$ in Eq. (9) with the new definition in Eq. (B1) makes Eqs. (10) - (13) applicable to this model, as well. Contributions from other evolutionary processes, such as gravitational wave radiation reaction; realistically prescribed stellar winds; tidal evolution, et c. can also be added. Each will make its own contribution to the angular momentum and total mass loss. For example, orbital decay by gravitational radiation reaction (Landau & Lifshitz, 1951) can be included as an other sink of angular momentum:

$$-\left.\frac{\partial L}{\partial t}\right|_{GR} = \frac{32G\mu}{5c^5}(GM_T)^6(L/\mu)^{-8}\ . \tag{B4}$$

In most cases, this type of physics can be modelled as an intrinsic $\dot{r}_L$ (the second term in Eq. (69)). Like the intrinsic stellar expansion term of Eq. (68), this kind of evolution occurs even in the absence of mass transfer. Therefore, the convenient change of variables from $t$ to $q$ used in Sect. (2) introduces singularities when evolution takes place in the absence of mass transfer. The equations of Sect. (2) still hold, but only for those phases of the binary's evolution durring which tidally-driven mass transfer takes place.

We temporarily neglect these complications and consider mass transfer via isotropic wind, isotropic re-emission, and formation of a ring, with mass fractions $\alpha$, $\beta$, and $\delta$ respectively. The remainder of the mass transfer (the fraction $\epsilon = 1-\alpha-\beta-\delta$) goes into accretion. The ratio $h_r/h_{bin}$ is $\gamma$, where $\gamma^2 = a_r/a$. Note that $\delta$, $\gamma$, $\beta$, and $\alpha$ are all used as before; $\epsilon$ should still be regarded as the accreted fraction.

$$\frac{M_T}{M_{T,0}} = \left(\frac{1+q}{1+q_0}\right)\left(\frac{1+\epsilon q_0}{1+\epsilon q}\right)\ , \tag{B5}$$

$$\frac{a}{a_0} = \left(\frac{q}{q_0}\right)^{2.\mathscr{A}-2}\left(\frac{1+q}{1+q_0}\right)^{1-2.\mathscr{B}}\left(\frac{1+\epsilon q}{1+\epsilon q_0}\right)^{3+2\mathscr{C}} \tag{B6}$$

$$\frac{P}{P_0} = \left(\frac{q}{q_0}\right)^{3.\mathscr{A}-3}\left(\frac{1+q}{1+q_0}\right)^{1-3.\mathscr{B}}\left(\frac{1+\epsilon q}{1+\epsilon q_0}\right)^{5+3\mathscr{C}} \tag{B7}$$

$$\mathscr{A}_5 = A\alpha+\gamma\delta \tag{B8}$$

$$\mathscr{B}_5 = \frac{A\alpha+\beta}{1-\epsilon} \tag{B9}$$

$$\mathscr{C}_5 = \frac{\gamma\delta(1-\epsilon)}{\epsilon}+\frac{A\alpha\epsilon}{1-\epsilon}+\frac{\beta}{\epsilon(1-\epsilon)} \tag{B10}$$

Taking $\alpha$, $\beta = 0$, gives formulae for a ring of strength $\delta$:

$$\frac{a}{a_0} = \left(\frac{q_0}{q}\right)^{2(1-.\mathscr{A}_r)}\left(\frac{1+q}{1+q_0}\right)\times\left(\frac{1+(1-\delta)q}{1+(1-\delta)q_0}\right)^{3+2\mathscr{C}_r} \tag{B11}$$

$$\frac{P}{P_0} = \left(\frac{q_0}{q}\right)^{3(1-.\mathscr{A}_r)}\left(\frac{1+q}{1+q_0}\right)\times\left(\frac{1+(1-\delta)q}{1+(1-\delta)q_0}\right)^{5+3\mathscr{C}_r} \tag{B12}$$

$$\frac{\partial \ln a}{\partial \ln q} = 2(.\mathscr{A}_r-1)+(1-2.\mathscr{B}_r)\frac{q}{1+q}+(3+2\mathscr{C}_r)\frac{q}{1+\epsilon q}\ , \tag{B13}$$

$$\frac{\partial \ln P}{\partial \ln q} = 3(.\mathscr{A}_r-1)+(1-3.\mathscr{B}_r)\frac{q}{1+q}+(5+3\mathscr{C}_r)\frac{q}{1+\epsilon q}\ . \tag{B14}$$

Where the relevant exponents are functions of the parameters $\gamma$ and $\delta$:

$$\mathscr{A}_r = \gamma\delta \tag{B15}$$

$$\mathscr{B}_r = 0 \tag{B16}$$

$$\mathscr{C}_r = \frac{\gamma\delta^2}{1-\delta} \tag{B17}$$

$$\epsilon_r = 1-\delta\ . \tag{B18}$$

It is also instructive to examine the model in the degenerate cases of $\epsilon = 0$ and $\epsilon = 1$, where the functional forms change. When there is no accretion ($\epsilon = 0$), the standard $\mathscr{C}_5$ becomes singular, while the term $1+\epsilon q$ approaches 1. Defining the singular part of $\mathscr{C}_5$:

$$\mathscr{C}_{sing} = \lim_{\epsilon\to 0}\epsilon\mathscr{C}_5 = \beta+\gamma\delta\ , \tag{B19}$$

the equations governing binary evolution can be rewritten, for the case when no material is accreted:

$$\frac{L}{L_0} = \left(\frac{q}{q_0}\right)^{\mathscr{A}_5}\left(\frac{1+q_0}{1+q}\right)^{\mathscr{B}_5}\exp\left[(q-q_0)\mathscr{C}_{sing}\right]\ , \tag{B20}$$

$$\frac{a}{a_0} = \left(\frac{q}{q_0}\right)^{2(.\mathscr{A}_5-1)}\left(\frac{1+q_0}{1+q}\right)^{1-2.\mathscr{B}_5}\exp\left[2\mathscr{C}_{sing}(q-q_0)\right]\ , \tag{B21}$$

$$\frac{P}{P_0} = \left(\frac{q}{q_0}\right)^{3(.\mathscr{A}_5-1)}\left(\frac{1+q_0}{1+q}\right)^{1-3.\mathscr{B}_5}\exp\left[3\mathscr{C}_{sing}(q-q_0)\right]\ , \tag{B22}$$

$$\frac{\partial \ln a}{\partial \ln q} = 2(.\mathscr{A}_5-1)+(1-2.\mathscr{B}_5)\frac{q}{1+q}+(3+2\mathscr{C}_{sing})q\ , \tag{B23}$$

**Table 5.** This reference table is divided into three parts. First are the model parameter definitions. An index of equations for the coeficients $\mathscr{A}$, $\mathscr{B}$, and $\mathscr{C}$, relevant to each particular model, follows. Last are the various formulae of orbital evolution derived in this paper

| | winds | ring | combined |
|---|---|---|---|
| $-\frac{\partial m_{mode}}{\partial m_2}$ | $\alpha, \beta$ | $\delta$ | $\alpha, \beta, \delta$ |
| $\epsilon = -\frac{\partial m_1}{\partial m_2}$ | $1-\alpha-\beta$ | $1-\delta$ | $1-\alpha-\beta-\delta$ |
| $\mathscr{A}$ | Eq. (25) | Eq. (B15) | Eq. (B8) |
| $\mathscr{B}$ | Eq. (26) | Eq. (B16) | Eq. (B9) |
| $\mathscr{C}$ | Eq. (27) | Eq. (B17) | Eq. (B10) |

$$\frac{M_T}{M_{T,0}} = \left(\frac{1+q}{1+q_0}\right)\left(\frac{1+\epsilon q}{1+\epsilon q_0}\right)^{-1} \quad \text{(Eq. (22))}$$

$$\frac{L/\mu}{L_0/\mu_0} = \left(\frac{q}{q_0}\right)^{\mathscr{A}-1}\left(\frac{1+q}{1+q_0}\right)^{1-\mathscr{B}}\left(\frac{1+\epsilon q}{1+\epsilon q_0}\right)^{\mathscr{C}+1}$$

$$\frac{P}{P_0} = \left(\frac{q}{q_0}\right)^{3.\mathscr{A}-3}\left(\frac{1+q}{1+q_0}\right)^{1-3.\mathscr{B}}\left(\frac{1+\epsilon q}{1+\epsilon q_0}\right)^{3\mathscr{C}+5}$$

$$\frac{a}{a_0} = \left(\frac{q}{q_0}\right)^{2.\mathscr{A}-2}\left(\frac{1+q}{1+q_0}\right)^{1-2.\mathscr{B}}\left(\frac{1+\epsilon q}{1+\epsilon q_0}\right)^{2\mathscr{C}+3}$$

$$\frac{\partial \ln a}{\partial \ln q} = 2(.\mathscr{A}-1) + (1-2.\mathscr{B})\frac{q}{1+q} + (2\mathscr{C}+3)\frac{\epsilon q}{1+\epsilon q}$$

$$\frac{\partial \ln P}{\partial \ln q} = 3(.\mathscr{A}-1) + (1-3.\mathscr{B})\frac{q}{1+q} + (3\mathscr{C}+5)\frac{\epsilon q}{1+\epsilon q}$$

$$\frac{\partial \ln P}{\partial \ln q} = 3(.\mathscr{A}_5-1) + (1-3.\mathscr{B}_5)\frac{q}{1+q} + (5+3\mathscr{C}_{sing})q\ . \quad \text{(B24)}$$

It might be worth noting that the above considerations are irrelevant for the pure $\alpha = 1$ models, where $\beta$, $\delta$, and $\epsilon$ vanish. There is no profound reason for this.

In the case where all material is accreted ($\epsilon = 1$), there are seeming singularities in the coeficients $\mathscr{B}_5$ and $\mathscr{C}_5$. Proper solution of the equations of evolution in this case, or setting $\epsilon q \rightarrow q$ before taking limiting values of the coeficients $\mathscr{B}_5$ and $\mathscr{C}_5$, shows that there is no problem at all. In this case, the equations reduce to Eqs. (32), (33), and:

$$M_T = M_{T,0}\ , \quad \text{(B25)}$$

$$L = L_0\ , \quad \text{(B26)}$$

$$\frac{\partial \ln a}{\partial \ln q} = 4\frac{q}{1+q} - 2\ , \quad \text{(B27)}$$

$$\frac{\partial \ln P}{\partial \ln q} = 6\frac{q}{1+q} - 3\ . \quad \text{(B28)}$$

## References


Banit, M., Shaham, J. 1992, ApJ, 388 L19
Bhattacharya, D., van den Heuvel, E.P.J. 1991, Phys. Rep. 203, 1
Blaauw, A. 1961, Bull. Astron. Inst. Neth., 15, 265
Clayton, D.D. 1968, Principles of Stellar Evolution and Nucleosynthesis, University of Chicago Press.
Eggleton, P.P. 1983, ApJ, 268, 368
Flannery, B.P., van den Heuvel, E.P.J. 1975, A&A, 39, 61
Frank, J., King, A.R., Lasota, J.P. 1992, ApJ, 385, L45
Frank, J., King, A.R., Raine, D.J. 1985, Accretion Power in Astrophysics, Cambridge University Press.
Ghosh, P., Lamb, F.K. 1978, ApJ, 223, L83
Hameury, J.M., King, A.R., Lasota, J.P., Raison, F. 1993, A&A, 277, 81
Harpaz, A., Rappaport, S. 1991, ApJ, 383, 739
Hjellming, M.S., Webbink, R.F. 1987, ApJ, 318, 794
Huang, S.S. 1963, ApJ, 138, 342
Iben, I. Jr., Tutukov, A.V. 1985, ApJS, 58, 661
Johnston, S., Manchester, R.N., Lyne, A.G., Bailes, M., Kaspi, V.M., Guojun, Q., D'Amico, N. 1992, ApJ, 387, L37
Johnston, S., Manchester, R.N., Lyne, A.G., D'Amico, N., Bailes, Gaensler, B.M., Nicastro, L. 1995, MNRAS, 279, 1026
Kelvin, Sir William Thomson, Lord. 1891-1894, Popular Lectures, Macmillan & Co.
King, A.R., Kolb, U. 1995 ApJ, 439, 330
Kochanek, C.S. 1993, ApJ 406, 638
Kulkarni, S.R., Narayan, R. 1988, ApJ 335, 755
Landau, L.D., Lifshitz, E.M. 1951, The Classical Theory of Fields, Addison-Wesley Press, Inc.
Lin, D.N.C., Papaloizou, J. 1979, MNRAS, 186, 799
London, R., McCray, R., Auer, L.H. 1981, ApJ, 243, 970
London, R.A., Flannery, B.P. 1982, ApJ, 258, 260
Melatos, A., Johnston, S., Melrose, D.B. 1995, MNRAS 275, 381
Paczyński, B. 1971, Ann. Rev. A&A, ARAA 9,183
Pennington, R. 1985, in Interacting Binary Stars, Pringle, J. E. and R. A. Wade, *eds.*, p197.
Podsiadlowski, Ph. 1991 Nat, 350, 136
Press, W.H., Flannery, B.P., Teukolsky, S.A., Vetterling, W.T. 1986, Numerical Recipes, Cambridge University Press.
Refsdal, S., Weigert, A. 1970 A&A, 6, 426
Ruderman, M., Shaham, J., Tavani, M. 1989, ApJ, 336, 507
Shore, S.N. 1994, in Interacting Binaries (Saas-Fee 22), Shore, S.N., et al., *eds.*, p1
Stix, M. 1991, The Sun, Springer Verlag.
Sweigart, A.V., Gross, P.G. 1978, ApJS, 36, 405
Taam, R.E. 1983, Ap. J, 270, 694
Tauris, T., 1996, A&A, 315, 453.
Tavani, M. 1991, ApJ 366, L27
Tavani, M., London, R. 1993, ApJ, 410, 281
van den Heuvel, E.P.J. 1994, in Interacting Binaries (Saas-Fee 22), Shore, S.N., et al., *eds.*, p263
van Kerkwijk, M.H., Charles, P.A., Geballe, T.R., King, D.L., Miley, G.K., Molnar, L.A., van den Heuvel, E.P.J. 1992, Nat, 355, 703
Verbunt, F. 1993, Ann. Rev. A&A, 31, 93
Verbunt, F., Phinney, E.S. 1995, A&A, 296, 709
Webbink, R.F. 1975 MNRAS, 171, 555
Webbink, R.F. 1985, in Interacting Binary Stars, Pringle, J.E. and R.A. Wade, *eds.*, p39.
Webbink, R.F., Rappaport, S., Savonije, G.J. 1983, ApJ, 270, 678


This article was processed by the author using Springer-Verlag LaTeX A&A style file *L-AA* version 3.